

JUMPS

The Journal of Undergraduate McGill Physiology Students

Edition 9 | 2017

The Journal of Undergraduate McGill Physiology Students

Edition 9: 2017

Published by the McGill Physiology Undergraduate League of Students

April 2017

Rights to data belong to the authors and/or their laboratories.

Reproduction prohibited

Formatting by Jiachen Liang

Cover Photo

Michigan Cancer Foundation-7 (MCF-7) cells in culture.

MCF-7 are primary breast adenocarcinoma cells expressing estrogen and progesterone receptors, mainly used in the study of invasive breast cancer.

Photo by Jiachen Liang

Cover design by Jamie Kim

Table of Contents

Editorial	1
Christina Kim	
Screening of Epigenetic Probes for the Treatment of Pediatric Glioblastomas in vitro	3
Hannah Kapur, Nada Jabado	
The effects of PIX mutations on the turnover rate of paxillin-containing focal adhesions	13
Aleksandar Borisov, Claire Brown	
Review of the Current State of Knowledge Regarding the Potential Functions of Neural Heterogeneities for Information Processing Within a Given Cell Type	21
Kavya Anchuri	
Author information	26
Editor information	28

Editorial

Dear members of the Department of Physiology,

It is my greatest pleasure to welcome you to the 9th edition of the Journal of Undergraduate McGill Physiology Students. Every year, JUMPS publishes the work of our very own Physiology students in an attempt to share their scientific findings with our colleagues, professors, and the public. Our aim is to recognize our fellow scientists and provide an opportunity for them to showcase their work to the interested public. During the publication process, my team, consisting of 7 editors, 3 authors, and 1 formatter, took a large step towards understanding the field of scientific research, specifically, how acquired data becomes everyday knowledge.

Science answers some the fundamental questions I had as a child—why do we live and why do we die? Science helped me understand how cells construct every tissue, organ, and muscle which in turn help me think, breathe and run. Understanding the foundation of all living things helps me comprehend the indiscernible relationships within the world around me. When cells function properly and harmoniously, the creation of life is possible, however, the slightest malfunction has the potential to put an organism at risk. The reasons for malfunction are many, and the authors showcased in this journal have investigated some of these, previously unexplained mechanisms, behind malfunction. Their contribution to knowledge advancement is exhilarating, and it is with immense pride that I share their work with you.

The well-established field of science is continuously changing, with a constant, and rapid, influx of novel information. Physiology research has provided the pillars of established, scientific knowledge, while at the same time, provides the most recent breakthroughs and discoveries, all of which prepare students in Physiology for their future careers. To be a member of a research institute at the cutting-edge of technology is truly a privilege.

However, much remains unknown. To give an example, it has been over 20 years since the discovery of the protein leptin, and yet, its mechanism of action remains a mystery. This inability to understand a certain type of disease or mutation can be discouraging, however, it also creates the potential for motivated scientists to flourish. Research is about looking for the “solvable” question in the unknown. The opportunities to make scientific contributions are everywhere in the Department of Physiology, and I encourage young students to become involved with the scientific community as early as possible.

I hope you enjoy reading the work of our colleagues and that science continues to help you understand our everyday life!

Sincerely,

Christina Joo Hyun Kim
JUMPS Editor-in-Chief 2017



Screening of Epigenetic Probes for the Treatment of Pediatric Glioblastomas *in vitro*

Hannah Kapur¹, Nada Jabado^{2,3}

¹ Department of Physiology, McGill University, Montreal, QC, Canada

² Department of Human Genetics, McGill University, Montreal, QC, Canada

³ Department of Pediatrics, Montreal Children's Hospital, McGill University Health Centre, Montreal, QC, Canada

ABSTRACT

Pediatric high-grade gliomas are highly aggressive brain tumours that are difficult to treat. Our lab previously discovered recurrent somatic mutations in histone 3 variant 3, involving the K27 and G34 residues on the histone tail, which tightly correlate with modification of the epigenome and alteration of chromatin architecture. The PRC2 complex is the exclusive methyltransferase for K27, and the K27M mutation restricts access of EZH2, the catalytic subunit, to its target substrate, leading to loss of K27 methylation globally. Small-molecule targeting, particularly that of epigenetic modifiers, has proven effective in many types of cancers and they constitute an important avenue for therapy. The objective of this project was to evaluate the efficiency and efficacy of epigenetic probes on patient-derived primary high-grade glioma cell lines. We used varying concentrations of methyltransferase PRC2 (GSK343 and UNC1999), histone demethylase (GSK-J4), and histone deacetylase (Panobinostat) inhibitors to generate cell viability dose-response curves for the following pediatric glioblastoma cell lines: BT245 (K27M-H3.3), HSJ-019 (K27M-H3.3), DIPG4 (K27M-H3.1), DIPG13 (K27M-H3.3), BT416 (K27M-H3.3), G477 (WT histone), pcGBM2 (WT histone), and KNS42 (G34V). Our results show that all of the cell lines respond to the probes, albeit with different kinetics. In particular, K27M mutated cell lines are more sensitive to the epigenetic probes, when compared to a WT histone glioblastoma. The differing kinetics between cell lines highlight the importance of studying the effects of these probes on cell cycle markers, as well as the association of the different histone marks with chromatin using chromatin immunoprecipitation sequencing (ChIPseq) analysis.

INTRODUCTION

Pediatric high-grade gliomas, which include glioblastomas (GBM) and diffuse intrinsic pontine gliomas (DIPG), are a highly malignant type of brain tumour in children¹. These tumours are morphologically indistinguishable from their adult counterparts, however, children show worse prognoses as they are largely unresponsive to the aggressive therapies used in adults. Previous research identified the molecular pathogenesis of pediatric GBM using whole-exome sequencing^{2,3}. This study revealed two recurrent mutations within the replication-independent histone H3.3 gene (*H3F3A*) in about 50% of cases, residing at K27

and G34 residues on the amino-terminal tail of H3.3. These mutations substitute lysine 27 with

methionine (K27M) and glycine 34 with arginine or valine (G34R/V). K27M mutations were also frequently found in DIPGs at both the replication-dependent histone H3.1 gene (*HIST1H3B*) and in H3.3²⁻⁴. Histone mutations were also identified in other cancers such as H3.3K36M and H3.3G34W/L in chondroblastomas and giant cell tumours of the bone, respectively⁵. These mutations were of interest because histone genes are highly conserved in eukaryotes and prior to this finding, no disorders had been associated with histone mutations. Additionally, this data suggests

that defects in chromatin architecture underlie pediatric high-grade glioma pathogenesis².

K27 and G34 histone mutations were found to be associated with tumour location and patient age. K27M-H3.3 mutations were mainly midline, thalamic, and DIPG tumours, and occurred in younger patients, with a median age of 11^{2,4}. K27M-H3.1 mutant DIPGs tend to occur in very young children⁶. G34R/V-H3.3 mutations were mainly in the cerebral hemispheres and occurred in older patients, with a median age of 20^{2,4}. Although these are considered driver mutations, they are often associated with partner mutations that are essential for inducing tumorigenesis². Patients with H3K27M mutant tumours have a poor prognosis and a shorter survival rate, prompting interest for further studies⁷.

Epigenetic regulation controls gene expression without altering the genetic code, and is mediated by specific and reversible modifications, such as methylation and acetylation of DNA and histone proteins to control the conformational transitions between active and inactive chromatin states⁸. These modifications are performed by enzymes, which have recently been identified as potential therapeutic targets for cancer⁷. Of interest to this study are the methylation modifications (mono-, di-, tri-methylation) performed at H3K27 residues exclusively by the EZH2 histone methyltransferase (HMT) subunit of the polycomb repressive complex 2 (PRC2), as it is essential in regulating the transcription of cancer-related genes⁹⁻¹¹. Histone demethylase (HMD) activity at H3K27 is performed by JMJD3/KDM6B and UTX/KDM6A. Additionally, acetyl modifications are also performed at this site by histone acetyltransferases (HAT) and histone deacetyltransferases (HDAC)⁷. H3K27M mutations cause global changes in the methylation and acetylation landscape, thus leading to changes in gene expression and tumorigenesis.

Lewis et al. identified gain-of-function activity in H3K27M mutant DIPGs by showing that H3K27M sequesters PRC2 histone methyltransferase, resulting in a dominant negative phenotype and suppressing PRC2 function globally¹². Interestingly, the mutations in these tumours are always heterozygous, and the effect of H3K27M in a single mutant allele can suppress the di- and trimethylation of wild-type (WT) H3K27^{1,12-15}. This results in transcriptional reprogramming of the cell, causing changes in gene expression. It has been previously described that genes with increased H3K27 trimethylation (H3K27me3) in H3K27M

mutant tumours are associated with cancer developmental pathways¹³.

Mutant oncoproteins have been a popular target for cancer therapy; however, therapeutic targeting of enzymes responsible for chromatin modifications and epigenetic regulation is a novel strategy^{4,16}. For this purpose, the objective of this project was to evaluate the efficiency and efficacy of new epigenetic probes on patient-derived primary high-grade glioma cell lines. We hypothesized that targeting epigenetic markers in pediatric high-grade gliomas will impair cell viability and potentially inhibit tumorigenesis. Specifically, H3K27 methyl and acetyl modifications were of interest and we targeted this site with specific EZH2-HMT, HMD, and HDAC inhibitors. We show that all patient-derived primary tumour cell lines respond to the epigenetic probes, albeit with differing kinetics. Additionally, we show that H3K27M mutated cell lines demonstrated higher sensitivity to the probes when compared to high-grade gliomas with no histone mutations. Future studies will allow us to examine the effects of these probes on cell cycle markers, as well as the association of the different histone markers with chromatin.

METHODS

Patient and Tumour Samples

All samples were obtained with informed consent after approval of the Institutional Review Board of the respective hospitals they were treated in, and independently reviewed by senior pediatric neuropathologists. BT245 (K27M-H3.3), HSJ-019 (K27M-H3.3), DIPG4 (K27M-H3.1), DIPG13 (K27M-H3.3), BT416 (K27M-H3.3), G477 (WT histone), pcGBM2 (WT histone), and SJG2 (WT histone) patient-derived primary tumour cell lines were used (Table 1).

CELL LINE	HISTONE MUTATION
BT245	K27M (H3.3)
HSJ-019	K27M (H3.3)
DIPG 4	K27M (H3.1)
DIPG 13	K27M (H3.3)
BT416	K27M (H3.3)
G477	WT
pcGBM2	WT
SJG2	WT

Table 1: Cell lines tested so far.

Epigenetic Probes

All the epigenetic probes were obtained from the Structural Genetic Consortium (SGC), Toronto. Table 2 summarizes the epigenetic probes tested. We used two histone methyltransferase (PRC2) inhibitors: (1) GSK343, competitive inhibitor with the cofactor SAM on the EZH1 or EZH2 subunit of PRC2; (2) UNC1999, a competitive inhibitor with the cofactor SAM and non-competitive inhibitor for the peptide substrate on the EZH1 or EZH2 subunit of PRC2. We also used UNC2400, an EZH2 inhibitor reduced-activity compound, as a negative control. We used one histone demethylase (UTX/JMJD3) inhibitor: GSKJ4, inhibitor of JMJD3 and UTX binding to substrate. We used one histone deacetylase inhibitor: Panobinostat, for which the mechanism of action is unknown. All drugs were prepared in 10 % dimethyl sulfoxide (DMSO).

DRUG	TARGET	CONCENTRATION
GSK343	SAM (EZH1/2)	0.5-1.5-2.5-3-3.5-4 (uM)
UNC1999	SAM (EZH1/2)	0.5-1.5-2.5-3-3.5-4 (uM)
UNC2400	EZH2 inhibitor non active compound	0.5-1.5-2.5-3-3.5-4 (uM)
GSK-J4	Histone demethylase (UTX/JMJD3)	0.5-1.5-2.5-3-3.5-4 (uM)
Panobino-stat (LBH-589)	HDAC	10-30-50-100-200-500 (nM)

Table 2: Epigenetic probes and dose ranges used

Cell Culture

BT245, HSJ-019, DIPG4, DIPG13, BT416, G477, and pcGBM2 cell lines were grown in Neurocult media supplemented with Neurocult NS-A proliferation supplement (Stem Cell technologies, Vancouver, CA) , EGF, FGF, heparin (Stem Cell technologies, Vancouver, CA), and a mix of antimycotic/antibiotic (Wisent Inc, Saint Bruno, QC, CA), and were plated in flasks pre-coated with poly-L-ornithine (Sigma, Oakville, ON, CA) and laminin (Invitrogen, Burlington, ON, CA). SJG2 cells were cultured in Dulbecco's modified Eagle's medium (Life technologies) supplemented with 10% FBS (ThermoFisher scientific, Burlington, ON,

CA), 1% penicillin-streptomycin (Wisent Inc, Saint Bruno, QC, CA), and 1% L-glutamine (Wisent Inc, Saint Bruno, QC, CA).

Drug Treatment and Cell Viability Assay

Cells were detached by scraping except for SJG2 cells that were detached by Trypsin/EDTA (Wisent Inc, Saint Bruno, QC, CA). 7,000 cells were plated in 96-well plates pre-coated with laminin. SJG2 cells were plated in uncoated plates. Cells were allowed to adhere for 24 hours. Serial dilutions were prepared in media for the following concentration ranges: 0.5uM, 1.5uM, 2.5uM, 3.0uM, 3.5uM, and 4uM for GSK343, UNC1999, GSKJ4, and UNC2400, and 10nM, 30nM, 50nM, 100nM, and 200nM for panobinostat. Cells were treated with the different dilutions in triplicate. 10% DMSO was added for untreated cells. Drugs were replenished every 3 days and the assay was performed for 7 days, as this is the amount of time required for epigenetic changes to take place. After 7 days, cell viability was assessed using alamarBlue reagent (ThermoFisher scientific, Burlington, ON, CA). This assay relies on a reduction reaction due to the reducing environment inside living cells, which converts Resazurin (blue) to Resofurin (red), thus giving a quantitative measure of cell viability. Absorbance was read by spectrophotometry after 6 hours at 570nm and 600nm. The following formula (Figure 1) was used to make dose-response curves. The equation of the curve was used to find the IC50 value, which is the concentration of probe needed for 50% inhibition, represented by the point of 50% cell viability.

$$\frac{(O2 * A1) - (O1 * A2) \times 100}{(O2 * P1) - (O1 * P2)}$$

Figure 1: O1: molar extinction coefficients of oxidized AB at 570nm (80586). O2: molar extinction coefficients of oxidized AB at 600nm (117216). A1: absorbance of test wells at 570nm. A2: absorbance of test wells at 600nm. P1: absorbance of positive control growth well (no test agent, vehicle) at 570nm. P2: absorbance of positive control growth well (no test agent, vehicle) at 600 nm.

Purified Histone Extraction

In order to check the effect of the epigenetic probes on the different histone marks, BT245, G477, and DIPG 4 cells were plated on 10 cm plates at 200,000 cells per plate. Cells were treated with GSK343 for 7 days, at the following IC₅₀ doses: 1.5uM for BT245, 2.5uM for G477, and 2.5uM for DIPG4. Extraction of histones was performed with the Epigentek extraction kit (Farmingdale, NY, US) following the manufacturer instruction. Protein quantification was performed using the BioRad Bradford protein quantification assay (BioRad, Mississauga, ON, CA).

Western Blot Analysis

4ug of histone extracts were run on 12% SDS-PAGE gels. Gel electrophoresis was run at 80V. Proteins were transferred on PVDF membranes at 100V for one hour. Membranes were blocked in 5% skimmed milk prepared in TBS supplemented with 0.1% Tween 20 (TBST). Then they were incubated overnight with the following primary antibodies total H3 (Cell Signaling Technologies, Danvers, MA, US), H3K27me3 (Cell Signaling Technologies, Danvers, MA, US), and K27M (Millipore, Etobicoke, ON, CA) at 1:100 dilutions. All antibodies were purchased from Cell Signaling. Membranes were washed three times in TBST, 15 minutes each, and incubated with goat anti-rabbit secondary antibody (GE Healthcare) at 1:5000 dilution. Digital imaging of blots was done using the Biorad Chemidoc Imaging system (BioRad, Mississauga, ON, CA).

RESULTS

Pediatric high-grade glioma cell lines respond with differing kinetics to the different epigenetic probes

H3K27M mutations lead to epigenetic changes that affect chromatin landscape and gene expression. Targeting these epigenetic changes may reverse tumorigenesis, and for this purpose we used GSK343, UNC1999, GSKJ4, and Panobinostat to target epigenetic regulators. We hypothesize that these epigenetic probes will rescue the H3K27M phenotype and inhibit tumorigenesis.

Pediatric glioma cells were plated in 96 well plates and treated for 7 days with the different drugs at the dose ranges described earlier. Cell viability was

assessed using the alamarBlue assay and the absorbance of each well was measured. A dose-response curve was generated and the results were expressed as a percent difference with vehicle treated wells. Figures 2 to 6 represent the cell viability dose-response curves for GSK343, UNC1999, UNC2400, GSK-J4, and Panobinostat, respectively.

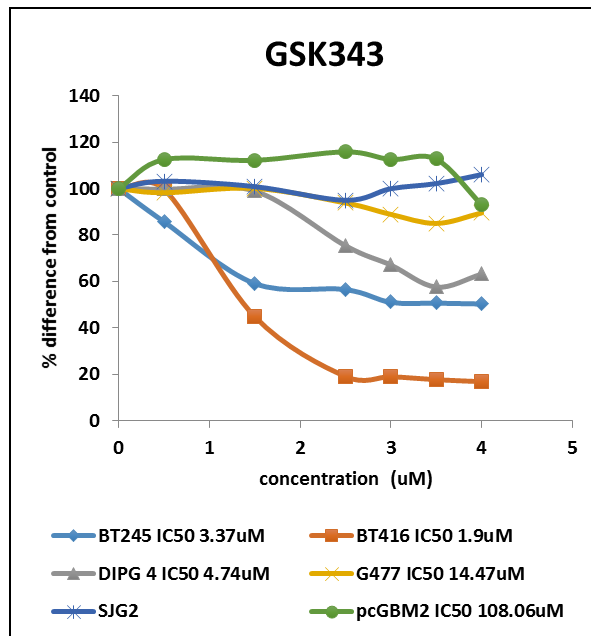


Figure 2: H3K27M cell lines show higher sensitivity to GSK343. Cell lines tested: BT245 (N=4), BT416 (N=2), DIPG4 (N=6), G477 (N=5), SJG2 (N=2), and pcGBM (N=1). Cells were treated with GSK343 for 7 days at the doses indicated in the methods. Cell viability was assessed with Alamar Blue. The results are expressed as percent changes from vehicle treated cells.

Each cell line responded differently to the epigenetic probes. GSK343, a histone methyltransferase inhibitor which targets the EZH1/2 catalytic subunit of the PRC2 complex, induced cell death at lower doses for BT416, BT245, and DIPG4, which are H3K27M cell lines, than for G477, and pcGBM2, the cell lines that do not present a histone mutation (WT). This was denoted by the IC₅₀ values: 1.94uM for BT416, 3.37uM for BT245, 4.74uM for DIPG4, 14.47uM for G477, and 108.06uM for pcGBM2 (Figure 2). Similarly, UNC1999, another histone methyltransferase inhibitor which targets the EZH1/2 catalytic subunit of the PRC2 complex, also induced a more potent response in the H3K27M cell lines, BT416, DIPG13, BT245, DIPG4, compared to the WT cell lines pcGBM2 and G477,

as demonstrated by the IC₅₀ values of 1.21uM, 2.32uM, 2.48uM, 3.85uM, 9.56uM, and 17.04uM, respectively (Figure 3). The SJG2 cells did not respond to the treatment.

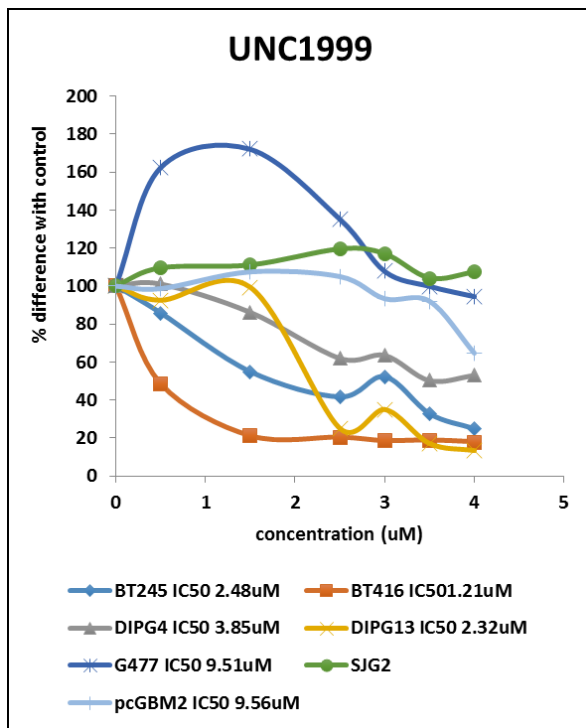


Figure 3: H3K27M cell lines show higher sensitivity to UNC1999. Cell lines tested: BT245 (N=3), BT416 (N=1), DIPG4 (N=6), DIPG13 (N=1), G477 (N=5), SJG2 (N=2), and pcGBM (N=1). Cells were treated with UNC1999 for 7 days at the doses indicated in the methods. Cell viability was assessed with Alamar Blue. The results are expressed as percent changes from vehicle treated cells.

To test whether the drugs were acting specifically on EZH2 as opposed to a non-specific effect, we tested the effect of UNC2400, a less active EZH2 inhibitor compound, as a negative control. The cells did not respond to the compound as demonstrated by the high IC₅₀ values, which confirms that the EZH2 inhibitors have a specific effect.

We also hypothesized that the maintenance of the methylation mark on H3K27 could repress gene expression and inhibit the transcription process, thus inhibiting tumorigenicity. For this purpose, we used the histone demethylase inhibitor, GSK-J4, which acts to target the UTX/JMD3 subunit of the lysine demethylase complex (KDM6) and prevent

substrate binding, thereby maintaining H3K27 methylation marks. Similarly, GSK-J4 induced different responses across the cell lines with a greater potency observed on BT245, BT416, HSJ-019, and DIPG4, the H3K27M cell lines, compared to SJG2, pcGBM2, and G477, the WT cell lines, as shown by the IC₅₀ values: 2.19uM for BT245, 2.32uM for BT416, 3.9uM for SJG2, 4.13uM for HSJ-019, 4.31uM for DIPG4, 4.83uM for pcGBM2, and 4.91uM for G477 (Figure 4).

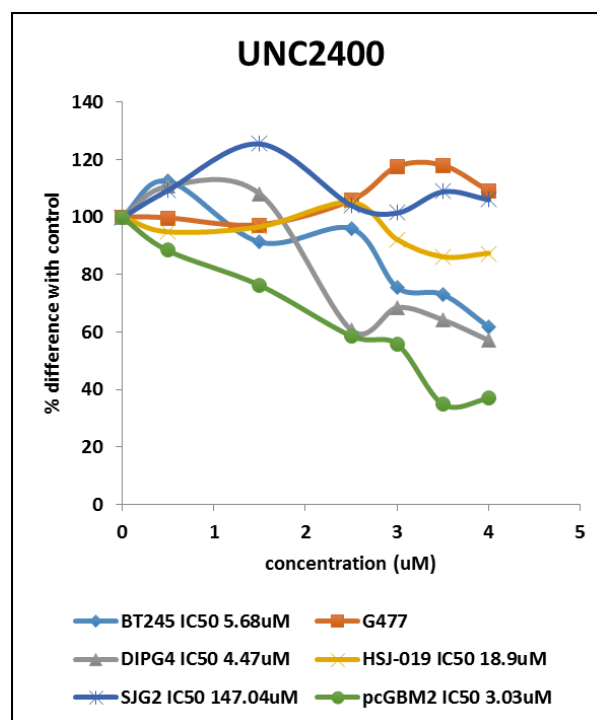


Figure 4: All cell lines show low response to the EZH2 inhibitor negative control UNC2400. Cell lines tested: BT245 (N=1), DIPG4 (N=2), HSJ-019 (N=1), G477 (N=2), SJG2 (N=1), and pcGBM (N=1). Cells were treated with UNC2400 for 7 days at the doses indicated in the methods. Cell viability was assessed with Alamar Blue. The results are expressed as percent changes from vehicle treated cells.

Previous research has identified that hyperacetylation corresponded with hypomethylation at H3K27 sites and the use of HDAC inhibitors has shown detoxifying effects by causing re-expression of anti-tumour genes¹². To test the effect of HDAC inhibitors, we used Panobinostat, an HDAC inhibitor that has been granted FDA-approval for treatment of DIPG and high-grade gliomas¹⁷. In response to Panobinostat, BT245, HSJ-019, pcGBM2, DIPG4, G477, DIPG13, and SJG2

demonstrated IC₅₀ values of 58.36nM, 72.76nM, 165.45nM, 215.97nM, and 247.48nM, 251.34nM, 336.87nM respectively (Figure 6). Again, we observed that H3K27M cell lines were more sensitive than WT cell lines.

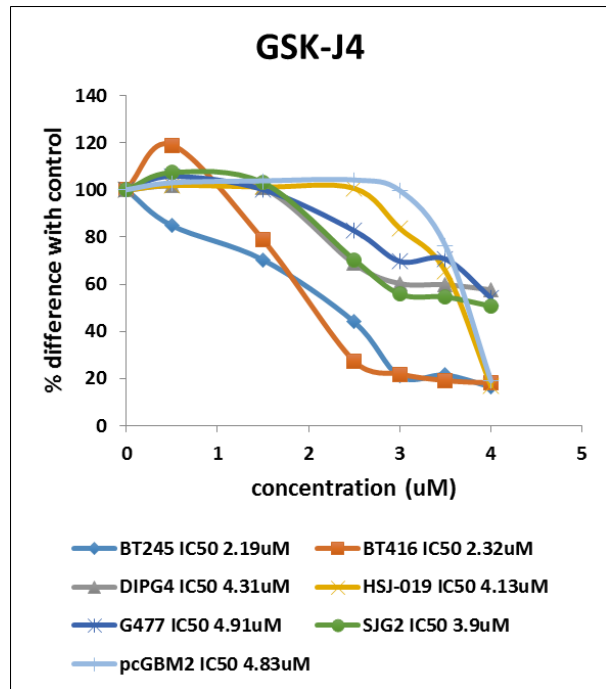


Figure 5: H3K27M cell lines show higher sensitivity to GSK343. Cell lines used: BT245 (N=3), BT416 (N=1), DIPG4 (N=5), HSJ-019 (N=2), G477 (N=4), SJG2 (N=2), and pcGBM (N=1). Cells were treated with GSK-J4 for 7 days at the doses indicated in the methods. Cell viability was assessed with Alamar Blue. The results are expressed as percent changes from vehicle treated cells.

These results show that the different drugs used had a more potent effect on the H3K27M cell lines compared to the WT cell lines, which responded at higher doses. Despite being more sensitive to the epigenetic probes than the non-mutated histone control, each of the H3K27M mutated cell lines responded to the drugs with differing kinetics, alluding to the possible effects of other mutations in the tumours and mutation location, such as on H3.1 or H3.3. However, additional cell lines with H3.1 and H3.3 mutations must be compared before conclusions can be made.

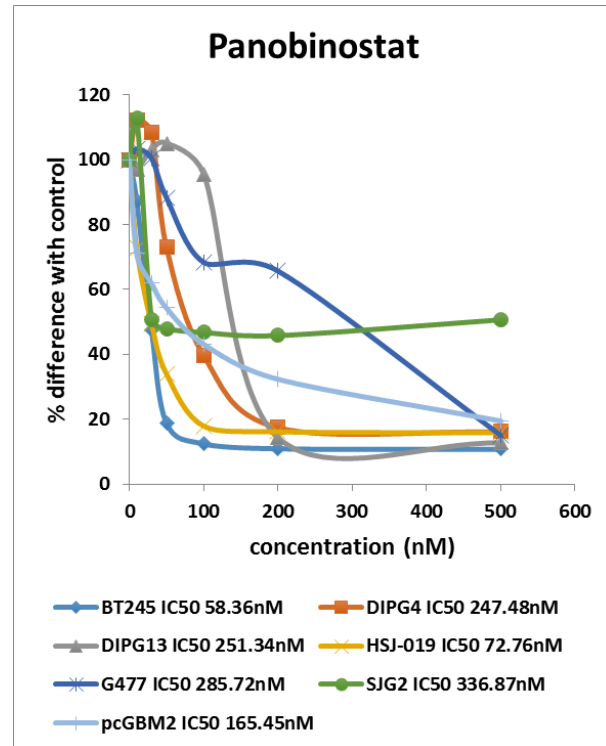


Figure 6: H3K27M cell lines show higher sensitivity to Panobinostat. Cell lines used: BT245 (N=1), DIPG4 (N=5), DIPG13 (N=1), HSJ-019 (N=2), G477 (N=5), SJG2 (N=1), and pcGBM (N=1). Cells were treated with Panobinostat for 7 days at the doses indicated in the methods. Cell viability was assessed with Alamar Blue. The results are expressed as percent changes from vehicle treated cells.

GSK343 reduces the level of H3K27me3 in G477 cells

In order to test whether the EZH2 inhibitor has an impact on H3K27me3 state, we performed western blot analysis on purified histones extracted from BT245, DIPG4, and G477 cell lines treated with GSK343 for 7 days (Figure 7) at the IC₅₀ concentrations or with DMSO only (vehicle control). There was no H3K27me3 detected for the BT245 and DIPG4 cell lines at any concentration of drug, confirming previous results regarding sequestering of the PRC2 complex due to H3K27M mutations, resulting in a global decrease in H3K27me3¹². We observed a decrease in H3K27me3 levels in G477 cells after 7 days, confirming that the drug targets the PRC2 complex and affects the methylation profile at the H3K27 residue. H3K27M marks were detected for the BT245 and DIPG4 cell lines, confirming presence

of the mutation. No H3K27M mark was detected in G477, as was expected because this GBM is WT for histone.

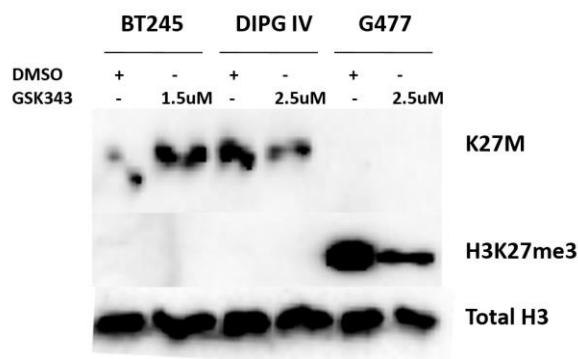


Figure 7: GSK343 (EZH2 inhibitor) decreases H3K27me3 levels in G477 cells treated for 7 days. BT245 and DIPG4 but not G477 cells express the H3K27M mutation. There is no expression of H3K27me3 in BT245 and DIPG4, in accordance with previously reported.

DISCUSSION

In this study, we demonstrated that epigenetic probes cause differential kinetic responses in each patient-derived tumour cell line. Furthermore, we show that H3K27M mutated cell lines act similarly in that they are more sensitive to the probes compared to their WT histone high-grade glioma counterparts. However, they do show differing kinetics from each other, despite being characterized with the same histone mutation status, suggesting that the presence of other mutations could be contributing to the differential response of the cell lines. It would therefore be useful to try different drug combinations in order to increase the efficiency of the response.

H3K27M mutated tumours demonstrate global hypomethylation, and previous studies have investigated the effect of increasing H3K27 methylation either by enhancing PRC2 methyltransferase activity or by inhibiting K27 demethylase activity⁷. A study by Hashizume et al. showed an anti-tumour effect when treating H3K27M DIPG tumour cell lines and Xenografts with GSK-J4, a JMJD3 histone demethylase inhibitor¹⁶. They observed increased H3K27me2 and H3K27me3, suppression of proliferative activity, and increased apoptosis specific to these H3K27M mutated cells, in addition to increased

survival in orthotopic xenografts. Similar results were also observed in T-cell acute lymphoblastic leukemia (T-ALL)¹⁸. Since PRC2 methyltransferase activity is suppressed, demethylase activity appears to be overactive at H3K27. GSK-J4 likely restores the balance between methyltransferase and demethylase activities, causing re-expression or enhanced expression of anti-tumour genes. As a result, JMJD3 inhibitors have emerged as a therapeutic epigenetic target⁷. Our results suggest a role of GSKJ4 in decreasing pediatric high-grade glioma viability, making it a potential candidate as an antitumor drug that should be studied further in *in vivo* models of pediatric high-grade gliomas.

H3K27 is also modified by histone acetylation, and Lewis et al. observed that hyperacetylation occurred alongside H3K27 hypomethylation¹². They demonstrated *in vivo* that transgenic H3.3K27M was enough to significantly increase K27 acetylation and significantly reduce H3K27me3. This suggests that K27 acetylation may also be responsible for glioma formation, and that methylation and acetylation should be studied in concert. Panobinostat, an HDAC inhibitor, has received FDA-approval for treatment of DIPG and other high-grade gliomas. It was found that inhibition of deacetylase activity “detoxifies” the H3K27M-induced inhibition of PRC2¹⁹. De-repression of PRC2 may cause re-expression of particular anti-tumour genes and normalize the H3K27M gene expression signature¹⁷. Our results show decreased viability in H3K27M cell lines when treated with Panobinostat. We observed this effect to be very potent compared to the other epigenetic probes used, indicated by IC50 values in the nanomolar ranges.

As previously mentioned, H3K27M mutated high-grade gliomas demonstrate a global decrease in H3K27 di- and trimethylation causing changes to the epigenetic landscape and gene expression. However, it was also observed that H3K27 trimethylation EZH2 was dramatically increased locally at many gene loci, and this increase at gene promoters was associated with expression of genes in various cancer pathways, such as p16Ink4A¹³. Thus, it is of interest to use inhibitors against EZH2 to diminish residual PRC2 activity and determine if re-expression of genes would be beneficial in the treatment of H3K27M tumours. To our knowledge, there is no data on the effects of GSK343 and UNC1999 in H3K27M mutated glioma cell lines. Our results show decreased viability in H3K27M cells treated with GSK343 and

UNC1999, therefore the mechanism and downstream effects of inhibiting PRC2 activity is of great interest.

Importantly, combinations of epigenetic probes may have therapeutic potential. For example, studies using a combination of GSK-J4 and Panobinostat suggested a synergistic effect against DIPG cells¹⁹. This combination counteracts the hypomethylation and hyperacetylation states of these tumours, thus it is of interest to this project to also investigate these combinations. Additionally, we could explore the possibility of inhibiting other subunits of PRC2 alone or in combination with EZH2 inhibitors in order to increase the potency of the drug effect. Disruption of EED, a PRC2 subunit, required for allosteric activation of the enzyme to propagate H3K27M trimethylation, has been found implicated in hematological malignancies²⁰. This provides evidence that EED is also involved in tumorigenesis and further experiments should test the effect of EED inhibitors.

It is essential to screen additional H3K27M mutated and WT cell lines in order to confirm these findings. In particular, a CRISPR-edited BT245 cell line reverted to wildtype could be used to observe if resilience to the probes could be restored. Further research should focus on understanding the mechanism of action of the epigenetic probes regarding changes in the DNA methylation profile, the association of chromatin with histone marks by ChIPseq analysis, the effect on the transcriptome, and the consequences on the cell cycle, such as the regulation of cell cycle markers including p16INK4a, P21, and p14ARF. Importantly, since many of the cell lines mentioned in this study have proven to induce tumors *in vivo* and are established models in our lab, it would be of key interest to study the effect of epigenetic probes on tumorigenicity *in vivo*.

CONCLUSIONS

The results provided in this work show that epigenetic probes could be a potential therapeutic agent in pediatric high-grade gliomas, however, the mechanism of their action is still poorly understood. Further work is needed in order to characterize their mechanism of action as well as their effect *in vivo*. It would be interesting to show whether epigenetic probes increase the sensitivity of the tumor to chemotherapy and radiotherapy

patients, and hence could be used in combination with these therapies to increase their efficiency.

ACKNOWLEDGEMENTS

The authors would like to thank Dr. Nada Jabado's postdoctoral fellow Michele Zeinieh for her mentoring as well as all lab members for their help and support throughout the project.

REFERENCES

1. Bender S, Tang Y, Lindroth AM, et al. Reduced H3K27me3 and DNA hypomethylation are major drivers of gene expression in K27M mutant pediatric high-grade gliomas. *Cancer cell*. 2013;24(5):660-672.
2. Schwartzentruber J, Korshunov A, Liu XY, et al. Driver mutations in histone H3.3 and chromatin remodelling genes in paediatric glioblastoma. *Nature*. 2012;482(7384):226-231.
3. Wu G, Broniscer A, McEachron TA, et al. Somatic histone H3 alterations in pediatric diffuse intrinsic pontine gliomas and non-brainstem glioblastomas. *Nat Genet*. 2012;44(3):251-253.
4. Khuong-Quang DA, Buczkowicz P, Rakopoulos P, et al. K27M mutation in histone H3.3 defines clinically and biologically distinct subgroups of pediatric diffuse intrinsic pontine gliomas. *Acta neuropathologica*. 2012;124(3):439-447.
5. Behjati S, Tarpey PS, Presneau N, et al. Distinct H3F3A and H3F3B driver variants define chondroblastoma and giant cell tumour of bone. *Nature genetics*. 2013;45(12):10.1038/ng.2814.
6. Roujeau T, Machado G, Garnett MR, et al. Stereotactic biopsy of diffuse pontine lesions in children. *Journal of neurosurgery*. 2007;107(1 Suppl):1-4.
7. Lulla RR, Saratsis AM, Hashizume R. Mutations in chromatin machinery and pediatric high-grade glioma. *Science advances*. 2016;2(3):e1501354.
8. Henikoff S. Nucleosome destabilization in the epigenetic regulation of gene expression. *Nat Rev Genet*. 2008;9(1):15-26.
9. Agger K, Cloos PA, Christensen J, et al. UTX and JMJD3 are histone H3K27 demethylases involved in HOX gene regulation and development. *Nature*. 2007;449(7163):731-734.
10. Broniscer A, Baker JN, Baker SJ, et al. Prospective collection of tissue samples at autopsy in children with diffuse intrinsic pontine glioma. *Cancer*. 2010;116(19):4632-4637.
11. Shen X, Liu Y, Hsu YJ, et al. EZH1 mediates methylation on histone H3 lysine 27 and complements EZH2 in maintaining stem cell identity and executing pluripotency. *Mol Cell*. 2008;32(4):491-502.
12. Lewis PW, Muller MM, Koletsky MS, et al. Inhibition of PRC2 activity by a gain-of-function H3 mutation found in pediatric glioblastoma. *Science*. 2013;340(6134):857-861.
13. Chan KM, Fang D, Gan H, et al. The histone H3.3K27M mutation in pediatric glioma reprograms H3K27 methylation and gene expression. *Genes & development*. 2013;27(9):985-990.

14. Ederveen TH, Mandemaker IK, Logie C. The human histone H3 complement anno 2011. *Biochim Biophys Acta*. 2011;1809(10):577-586.
15. Venneti S, Garimella MT, Sullivan LM, et al. Evaluation of histone 3 lysine 27 trimethylation (H3K27me3) and enhancer of Zest 2 (EZH2) in pediatric glial and glioneuronal tumors shows decreased H3K27me3 in H3F3A K27M mutant glioblastomas. *Brain pathology (Zurich, Switzerland)*. 2013;23(5):558-564.
16. Hashizume R, Andor N, Ihara Y, et al. Pharmacologic inhibition of histone demethylation as a therapy for pediatric brainstem glioma. *Nat Med*. 2014;20(12):1394-1396.
17. Grasso CS, Tang Y, Truffaux N, et al. Functionally defined therapeutic targets in diffuse intrinsic pontine glioma. *Nat Med*. 2015;21(6):555-559.
18. Ntziachristos P, Tsirigos A, Weistead GG, et al. Contrasting roles of histone 3 lysine 27 demethylases in acute lymphoblastic leukaemia. *Nature*. 2014;514(7523):513-517.
19. Brown ZZ, Muller MM, Jain SU, Allis CD, Lewis PW, Muir TW. Strategy for "detoxification" of a cancer-derived histone mutant based on mapping its interaction with the methyltransferase PRC2. *Journal of the American Chemical Society*. 2014;136(39):13498-13501.
20. Ueda T, Sanada M, Matsui H, et al. EED mutants impair polycomb repressive complex 2 in myelodysplastic syndrome and related neoplasms. *Leukemia*. 2012;26(12):2557-2560.

The effects of PIX mutations on the turnover rate of paxillin-containing focal adhesions

Aleksandar Borisov¹, Claire Brown^{1, 2}

¹ Department of Physiology, McGill University, Montreal, QC, Canada

² Life Sciences Complex Advanced BioImaging Facility, McGill University, Montreal, QC, Canada

ABSTRACT

Assembly and disassembly of adhesions, also called adhesion turnover, is regulated by multiple mechanisms. Here, the role of the PAK-interactive exchange factor (PIX) protein in adhesion turnover is exemplified, along with how mutations in its domains can either have no effect, or a significant effect in the efficiency of cell adhesion turnover. PIX is a protein that is part of a trimolecular complex shown to localize at the leading edges of cells and is part of the process that involves p21-activated kinase (PAK) induced phosphorylation of serine residue 273 on paxillin, which is important for regulating adhesion turnover. The mutants tested in this study included a PIX-ΔGBD mutant, which is a PIX protein that cannot bind to the G protein-coupled receptor kinase-interacting protein 1 (GIT1), a PIX-ΔSH3 mutant which is unable to bind PAK, and a PIX-LL mutant, which is a PIX protein lacking GTPase activity. The PIX-ΔGBD condition behaved similarly to the control group, with a slight decrease in the rate of adhesion turnover, possibly due to the experimental techniques used and the stress the cells underwent during imaging. However, these cells retained a relatively similar phenotype, suggested to be a result of GIT1 overexpression and localization at the leading edge by chance. The PIX-ΔSH3 condition showed a significant decrease in cell adhesion turnover rate, showing that PIX interaction with PAK is crucial for faster cellular protrusions. Lastly, the PIX-LL mutant condition also resulted in a significant decrease in cell turnover rate, showing that perhaps there is no effective compensatory mechanism for a GTPase knockout in this particular trimolecular complex.

INTRODUCTION

Cell migration is a vital area of research due to its importance with respect to cancer, wound healing, and embryonic development among other important cellular processes. A cell's ability to migrate allows it to access different tissues by upregulating or downregulating the activity of certain proteins. Migration is a normal part of development and wound healing, but goes awry during cancer metastasis. Cancer metastasis in particular is important because it involves the extra-vasation of a detached group of tumor cells or even an individual cell from a primary tumor into the bloodstream¹. These cancer cells can then

migrate to secondary sites as the cancer metastasizes. Cellular migration is measured by a scalar value of cell speed which is based on whole cell migration assays, and the assembly and disassembly of focal adhesions underlie the regulation of gross cellular movement. Focal adhesions are macromolecular protein complexes² that can consist of over 200 transmembrane, extracellular and intracellular proteins³ that help connect the extracellular matrix to the actin cytoskeleton inside the cell. It has been shown that the size of adhesions can be used to predict the speed of a cell². The idea that the size of focal adhesions predicts the speed of a cell comes from the fact that fast cells such as those of myeloid

lineage have small, short-lived focal adhesions whereas slower cells such as fibroblasts and endothelial cells have large, prominent adhesions².

The protein paxillin is known to be associated with focal adhesions and acts as an adaptor protein with multiple domains that serve as docking sites for tyrosine kinases, serine/threonine kinases, GTPase activating proteins (GAPs), cytoskeletal proteins, and other adapter proteins⁴. Its ability to localize to focal adhesions allows it to play an important role in the assembly and disassembly of adhesions through its interaction with adhesion-related proteins⁵ (Figure 1). Paxillin interacts with these proteins through its N terminal LD domains, C terminal LIM domains, and SH3 and SH2 domains⁵ (Figure 2). Further proof that paxillin is a

regulator of adhesion turnover is that paxillin knockout cells have shown impaired protrusion and disassembly⁶.

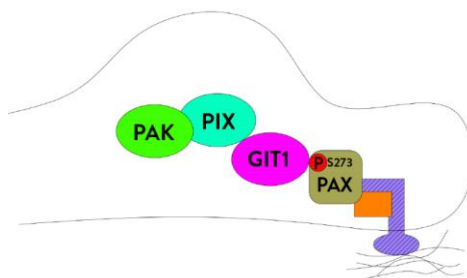


Figure 1: Molecular assembly of the paxillin-GIT1-PIX-PAK complex

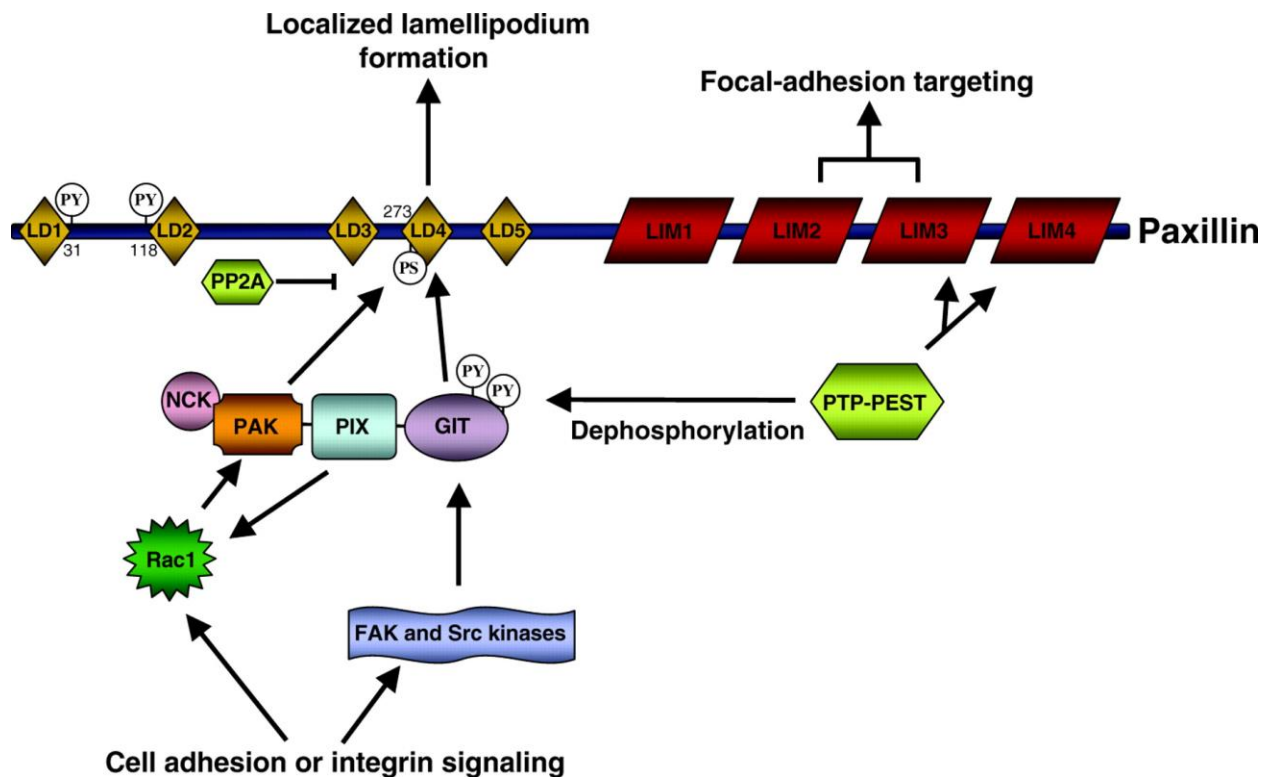


Figure 2: Paxillin protein map ¹¹

GIT1 is a regulator of cellular protrusions, interacts with the LD4 domain on paxillin, and offers a link between cellular protrusions and adhesion turnover. It plays a role in vesicle trafficking, cytoskeleton reorganization and targeting p21 activated kinase (PAK) to adhesions⁵. Research has shown that GIT1 likely interacts with paxillin via its serine residue 273 domain⁵ which is phosphorylated by PAK. Furthermore, GIT1 also interacts with a Rac exchange factor called PAK-interactive exchange factor (PIX) via its Spa2 homology domain (SHD). PIX is a rho-family guanine nucleotide exchange factor that also binds the Rac effector PAK⁵. The result is a GIT1-PIX-PAK complex, the localization of which to the leading edge of cellular protrusions has been shown to be coupled to dynamic cell movement.

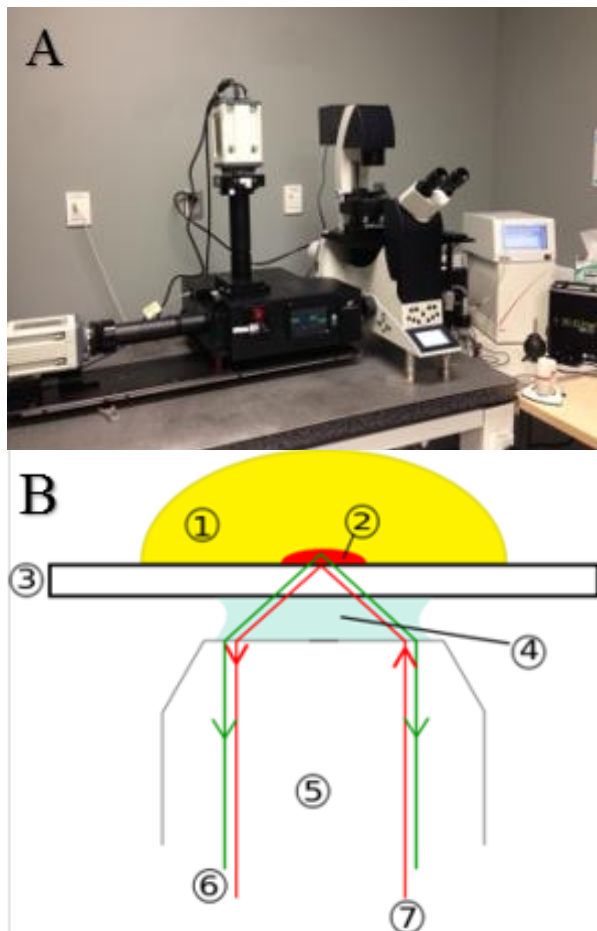


Figure 2: A: TIRF microscope at the ABIF facility at McGill. B: Example of how a TIRF microscope works. 1. Specimen 2. Evanescent wave range 3. Cover slip 4. Immersion Oil 5. Objective 6. Emission beam 7. Excitation beam

This study in particular focuses on the PAK-interactive exchange factor (PIX), and the working hypothesis that PAK is linked to paxillin via PIX⁵ (Figure 1). The interaction of GIT1-PIX-PAK near the leading edge of cells is required for Rac activation and adhesion turnover. The goal here was to test whether a GIT1-PIX-PAK interaction is required for fast adhesion dynamics. To do this an S273-paxillin EGFP fusion was transfected into CHO-K1 cells along with wild type or mutant forms of PIX mCherry fusions. The mutants tested were 1) PIX-ΔSH3 – a PAK binding deficient mutant, 2) PIX-ΔGBD – a GIT1 binding deficient mutant, and 3) PIX-LL – a GTPase activity deficient mutant. Based on previous studies, it was expected that CHO-K1 cells expressing PIX-ΔSH3, or PIX-LL would show less, and slower protrusiveness⁵ and stable, large adhesions as compared to the WT cells⁷. Conversely, the cells expressing PIX-ΔGBD should offer similar results to the WT-PIX control, likely due to PIX mislocalization⁸.

The microscope used to image the PIX mutants was a total internal reflection fluorescence (TIRF) microscope (Figure 3). A TIRF microscope produces an evanescent wave that only illuminates fluorophores up to ~ 100nm from the microscope slide. This wave is only generated when the incident light hits the interface at a high angle and is totally reflected at the glass-water surface. Two important benefits of TIRF microscopy for this project were that it offered a high signal-to-background noise ratio, and that it allowed imaging of events occurring at the plasma membrane, i.e. adhesion dynamics.

METHODS

Polymerase Chain Reaction

To create the plasmids used for fluorescent protein fusion transfection, PCR was performed in 4 MicroAmp reaction tubes (Corning, N8010540). 1 μ L of 0.1 μ g/ μ L SH3 PIX mutant, 1 μ L of each of 4 primers (designed by and obtained from Integrated DNA Technologies – for β-PIX: 5'-CGG GGT ACC GCC GCG ATG ACT GAT AAC A-3' and 5'-TCC CCC CGG GCT ATA GAT TGG TCT CAT CC-3', and for PAK1: 5'-CGG GGT ACC GCC GCG ATG TCA AAT AAC G-3' and 5'-TCC CCC CGG GTC AGT GAT TGT TCT TGG TT-3'), 1 μ L of dNTP's and 5 μ L Thermopol reaction buffer (NEB, B9004S) were added to each tube. 2 μ L MgSO₄ and 39 μ L of distilled water were added to two

tubes, along with 41 μL of distilled water to two other tubes. To prevent evaporation and condensation on the tube caps, 30 μL of mineral oil was added to each of the tubes. 1 μL of Vent Polymerase (NEB, M0254S) was added and the PCR reaction was quickly run thereafter. To purify the mixture after the PCR, the contents of the tubes were pipetted on to parafilm three times to dissolve as much oil as possible. Afterwards, the contents were transferred to new tubes, and 6 μL of gel loading dye was added to each tube. The digestion sites were confirmed with 1% agarose gel electrophoresis.

Transfection

A day prior to transfecting the plasmids, CHO-K1 PAX-E-GFP Wild Type cells were split and allowed to grow overnight to approximately 85% confluence. The next day the four plasmids – WT PIX, Δ GBD, Δ SH3, and LL were introduced to the four groups of cells. 140 μL of optimum reduced serum media and 10 μL of lipofectamine (ThermoFisher, 11668019) were added to each of four falcon tubes (Corning, 21008-918). In four other falcon tubes, 10 μL of each of the four plasmids was added along with 140 μL of optimum reduced serum media per tube. The first four tubes containing the CHO-K1 cells were mixed with the next four containing the plasmids with an Eppendorf by pipetting up and down and were given 25 minutes to mix.

The media was aspirated from the cells and the wells were washed twice with PBS. Then 2 mL of optimum media was added to each of the three wells, and the entire 300 μL mixture of plasmids of each of the treatments to one of the four wells. The cells were incubated for 6 hours with the plasmids. Lastly, the plasmid solution was aspirated from the wells, the cells were washed twice with PBS, and 2 mL of full DMEM low glucose media containing G418 antibiotic (ThermoFisher, 10567014) was added to each well.

Plating Cells for Turnover Assay

PBS (ThermoFisher, 10010023) and fibronectin (Sigma, F0895-1MG) were mixed at a ratio of 2 $\mu\text{g}/\text{mL}$ of fibronectin coating to PBS and vortexed in a falcon tube. 1.5 mL of the fibronectin mixture was added to each of four 35 mm cover glass bottom dishes (ThermoFisher, 150680) and they were incubated for one hour at 37°C so they would be coated with fibronectin. The fibronectin solution was aspirated and the dishes were washed three

times with PBS. The cells were split and plated on the fibronectin coated 35 mm dishes and incubated overnight until they were about 85% confluent.

Adhesion Turnover Assay

Prepared cells were placed on the microscope in a live incubation chamber at 37°C, with 5% humidified CO₂ with a gas flow at 40 mL/min. The TIRF laser was a 488nm diode laser set to 10% power. EGFP paxillin in the cells were imaged with a Hamamatsu ImageEM camera (Hamamatsu, Japan), with an exposure time of 150ms, the electron multiplication (EM) gain at 200, and the digitizer at 11MHz. The cells were given 10 minutes to acclimate on the microscope, and all imaging was acquired using a 63X/1.47 NA-oil immersion Leica objective. The focal plane of the cells was found using the EGFP channel, followed by which the cells expressing mCherry PIX were found using the eye piece. TIRF mCherry mode was used to center the cell to prepare it for acquisition. The mCherry was imaged using a 561nm diode laser set at 10% power, with the Hamamatsu ImageEM camera set at an exposure time of 150ms, the EM gain at 200, and the digitizer at 11MHz.

MetaMorph software multidimensional acquisition was used to obtain an image every 30 seconds for 27 minutes for a total of 55 image frames, and any drifting of the focus was adjusted between acquisition frames. The raw image files were saved as MetaMorph stack files.

Image Analysis

Image analysis was performed using MetaXpress 5.0 software (Molecular Devices, Sunnyvale, CA). A MetaMorph TIFF stack was opened in the software and a journal loop was created to perform a statistical background correction on each plane in order to zero the background. The background corrected file was saved as a MetaMorph stack and then opened in Imaris 7.5.2 (Bitplane - Zurich, Switzerland) as an image vs time series. The following steps led to obtaining the adhesion dynamic data:

1. The surfaces tab was opened and “segment region of interest” and “track surfaces over time” were selected.
2. A region of interest was selected (note: multiple regions of interest were sometimes included).

3. The surface area detail level was set to 0.25 μm and background subtraction was set to 0.25 μm .
4. The intensity threshold histogram was adjusted to encompass all the adhesions of interest.
5. In part 5 of 8, all the filters were deleted.
6. The max distance to look for adhesions was set to 2 μm and the max gap size to 3.
7. This step was skipped.
8. Finally “execute final calculations” was selected.

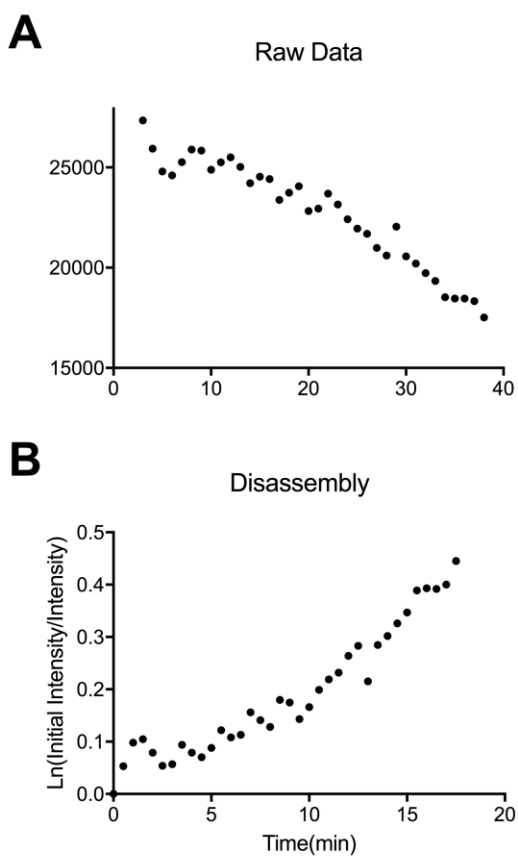


Figure 4: A: Sample raw data with raw intensity in arbitrary values as a function of time. B: Sample of data obtained from an area of disassembly with $\ln(\text{initial intensity}/\text{intensity})$ as a function of time (min).

To extract the data, the statistics tab was opened, under “detailed”, then “intensity mean”, and the data was logged in an Excel file. The Excel data was analyzed using a macros program which was written to plot the raw intensity vs time curves (Figure 4A), and each curve was analyzed for

areas of assembly (increasing intensity) and disassembly (decreasing intensity) (Figure 5). These areas were specifically selected from the entire data set. The areas of assembly were plotted using another macros program to plot $\ln(\text{intensity})/\text{initial intensity}$ vs time. To keep the slopes at positive rates the adhesions that were undergoing disassembly were plotted as $\ln(\text{initial intensity})/\text{intensity}$ vs. time (Figure 4B). The slopes obtained from these natural log plots were directly proportional to the assembly or disassembly rates, and the threshold used for a good fit to the data was an r score of 0.7.

RESULTS

The experiment was performed in triplicate, and each time three cells were analyzed for each of the WT/ Δ GBD/ Δ SH3/LL conditions. From each cell, 10 assembling focal adhesions and 10 disassembling focal adhesions were analyzed, equaling a total of 90 adhesions measured for each condition studied. Figure 6A-C shows a cell imaged for EGFP paxillin from the PIX- Δ SH3 condition at three time points: 0, 27 and 55 (corresponding to 0, 13.5 and 27 minutes after beginning of imaging). Each of the images represent expressed paxillin in each condition and the effect of the different PIX mutants on motility is what was studied. When compared to the cells expressing wild type PIX (Figure 6D-F), it can be seen that the adhesions were larger and more prominent. In fact, there were many more large adhesions in the central regions of the cells as well. The results of the adhesion dynamics measurements are summarized in Figure 7A and B which plot the average rates per minute for paxillin dynamics for all four PIX mutants’ assembly and disassembly rates. To examine significance, each condition was compared to the wild type PIX results in both the assembly and disassembly groups. There was no significant difference between the WT-PIX (adhesion assembly rate of 0.051/min) and the PIX- Δ GBD mutant in adhesion assembly rate (0.048, $p > 0.05$), while the disassembly rate of PIX- Δ GBD (0.045) was slightly lower than the WT-PIX (0.056, $p < 0.05$). Both assembly (0.0234, $p < 0.001$) and disassembly (0.0201, $p < 0.0001$) rates of the PIX- Δ SH3 mutant were significantly slower than those of the WT-PIX values. Similarly, the PIX-LL mutant exhibited a significantly lower adhesion turnover rate relative to the WT-PIX expressing cells, as their assembly rate was 0.0216 and their disassembly rate was 0.0215 with p values of < 0.0001 .

DISCUSSION

Our results showed that the assembly and disassembly of adhesion proteins at the protruding edge of cells dictate the speed of adhesion turnover. This observation that the localization of the PAX-GIT1-PIX-PAK module regulates Rac activity and therefore cellular protrusions is consistent with previous studies^{3, 5, 9}. The findings also support previous studies that the role of PIX in binding the Rac effector PAK and indirectly linking it to paxillin is crucial for fast adhesion turnover.

The PIX-ΔGBD mutants exhibited a similar phenotype to the WT-PIX condition, the explanation for which is a possible combination of mislocalization and overexpression^{7, 10}. It is thought that the PIX molecule can still bind PAK1 and activate it, despite not being recruited to the adhesion directly and because of its high expression levels it can still carry out its function, showing that its localization is not crucial. One possible reason for the significance found in the

slight decrease of adhesion disassembly rate of the PIX-ΔGBD mutant is that the experimental process of preparing the cells, along with imaging with a laser microscope could have damaged other cellular mechanisms. However, it is important to note that such an experimental pitfall could have also altered any of the other treatments. The PIX-ΔSH3 mutant, which is a PAK1 binding deficient mutant, and the PIX-LL – GTPase activity deficient mutant both showed a significantly lowered cell adhesion turnover rate, along with a phenotype of larger adhesions, consistent with studies from Nayal et al. and Koh et al.^{5, 8}.

In a pharmacological context, the importance of this study points towards the potential creation of drugs to target these domains on PIX in an attempt to alter the velocity of cellular movement. These small, dynamic adhesions and the proteins which constitute them and drive the movement of highly motile cells should continue to be studied in the hopes of further understanding the molecular mechanisms through which they interact.

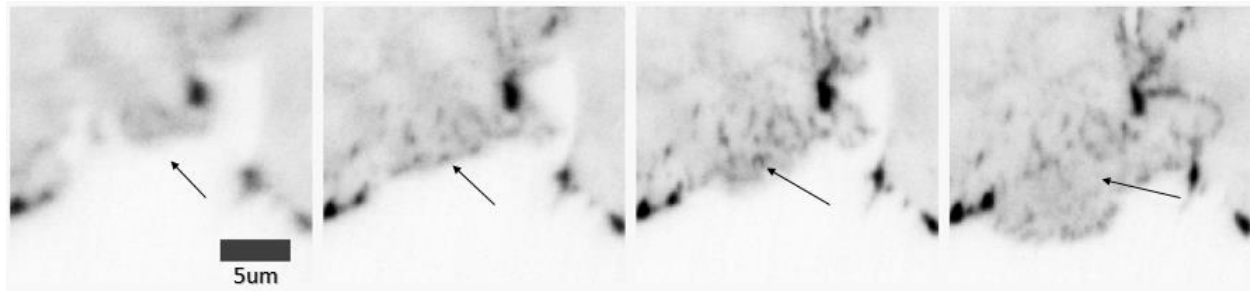


Figure 5: Invert image of EGFP paxillin from a WT PIX cell at time points 9, 15, 17 and 25 (corresponding to 4.5, 7.5, 8.5 and 12.5 minutes after the start of imaging). The arrow indicates an adhesion that assembles and disassembles during this time.

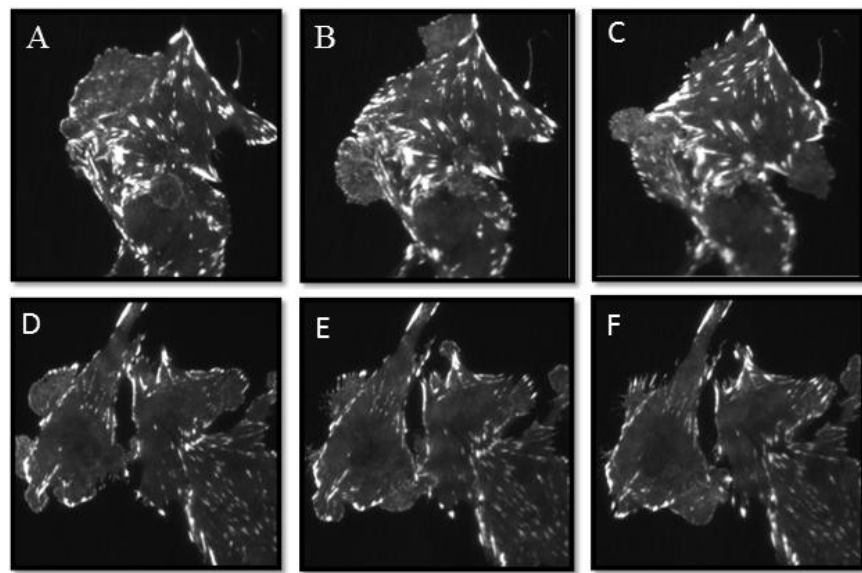


Figure 6: **A-C:** SH3 PIX mutant imaged for EGFP paxillin at time points 0, 27, and 55 which corresponds to 0, 13.5 minutes, and 27 minutes after the start of imaging. **D-E:** 3 WT PIX cells imaged for EGFP paxillin at time points 0, 27, and 55.

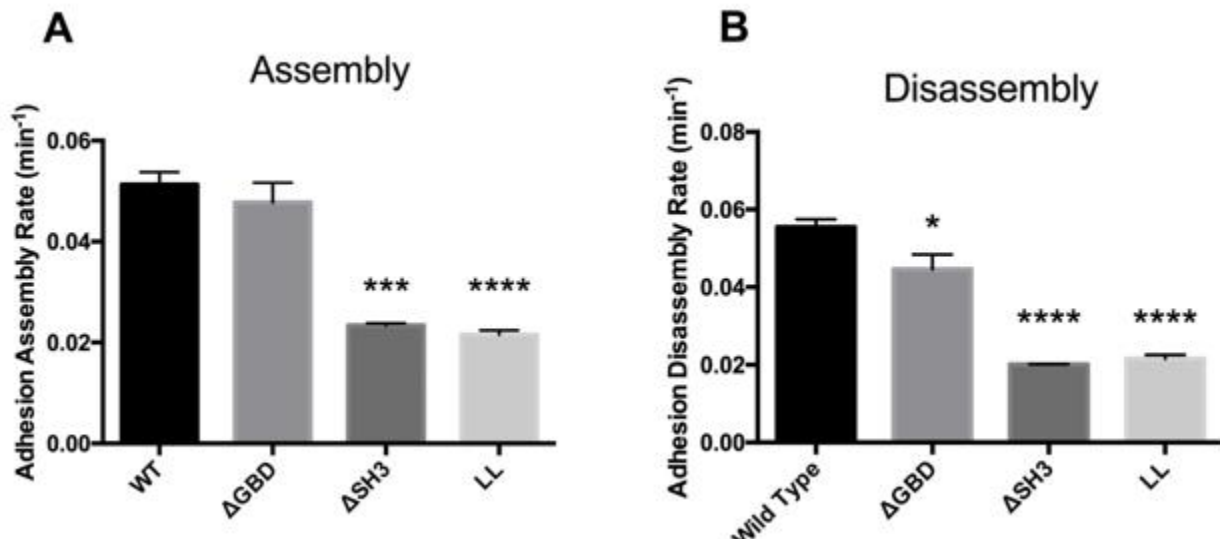


Figure 7: Significance found relative to the wild type PIX expressing cells. **A:** WT: 0.051, ΔGBD : 0.048, ΔSH3 : 0.0234, LL: 0.0216. **B:** WT: 0.056, ΔGBD : 0.045, ΔSH3 : 0.0201, LL: 0.0215. The error bars represent the standard error of the mean. Three experiments, $n=3$ cells and 90 adhesions

REFERENCES

1. Parsons, J. T., Horwitz, A. R., & Schwartz, M. A. (2010). Cell adhesion: integrating cytoskeletal dynamics and cellular tension. *Nature Reviews Molecular Cell Biology*, 11(9), 633–643.
2. Kim, D.-H., & Wirtz, D. (2013). Focal adhesion size uniquely predicts cell migration. *The FASEB Journal*, 27(4), 1351–1361.
3. Kuo, J.-C. (2013). Mechanotransduction at focal adhesions: integrating cytoskeletal mechanics in migrating cells. *Journal of Cellular and Molecular Medicine*, 17(6), 704–712.
4. Schaller MD. (2001) Paxillin: a focal adhesion-associated adaptor protein. *Oncogene*, 20(44), 6459-6472.
5. Nayal, A., Webb, D. J., Brown, C. M., Schaefer, E. M., Vicente-Manzanares, M., & Horwitz, A. R. (2006). Paxillin phosphorylation at Ser273 localizes a GIT1-PIX-PAK complex and regulates adhesion and protrusion dynamics. *The Journal of Cell Biology*, 173(4), 587–589.
6. Webb, D.J., Donais, K., Whitmore, L.A., Thomas, S.M., Turner, C.E., Parsons, J.T., Horwitz, A.F. (2004). FAK-Src signaling through paxillin, ERK and MLCK regulates adhesion disassembly. *Nat Cell Biol*, 6(2), 154-161
7. Zhang, H., Webb, D. J., Asmussen, H., & Horwitz, A. F. (2003). Synapse formation is regulated by the signaling adaptor GIT1. *The Journal of Cell Biology*, 161(1), 131–142.
8. Koh, C.G., E. Manser, Z.S. Zhao, C.P. Ng, and L. Lim. 2001. Beta1PIX, the PAK-interacting exchange factor, requires localization via a coiled-coil region to promote microvillus-like structures and membrane ruffles. *J. Cell Sci.* 114:4239–4251.
9. Kraynov, V.S., C. Chamberlain, G.M. Bokoch, M.A. Schwartz, S. Slabaugh, and K.M. Hahn. 2000. Localized Rac activation dynamics visualized in living cells. *Science*. 290:333–337.
10. Nagasaki A., Kanada M., Uyeda T. Q. P. (2009) Cell adhesion molecules regulate contractile ring-independent cytokinesis in Dictyostelium discoideum. *Cell Res.* 19, 236–246
11. Deakin N., Turner E., Paxillin comes of age. *J. Cell Sci.* 121:2435–2444.

Review of the Current State of Knowledge Regarding the Potential Functions of Neural Heterogeneities for Information Processing Within a Given Cell Type

Kavya Anchuri ¹

¹ Department of Physiology, McGill University, Montreal, QC, Canada

INTRODUCTION

The nervous system processes sensory information from an organism's surroundings in order to generate appropriate behavioural and physiological responses. Neurons encode the myriad features of sensory stimuli by means of intrinsic properties such as mean firing rate, receptive field location and size, stimulus selectivity, baseline firing, response amplitude, etc.¹ No two neurons will respond to identical stimuli in an identical manner, even if they belong to the same cell type. Heterogeneities among intrinsic properties of a given neuron type are ubiquitous in the nervous system, and have been documented in many contexts.²⁻⁶ Therefore, current research is focused on elucidating the functions of these neural heterogeneities in regards to processing sensory information. This review aims to address our current understanding of the functions of neural heterogeneities, and will discuss the roles of neural heterogeneities in population coding, information throughput, burst activity, envelope coding, and excitatory versus inhibitory control. All relevant data was sourced from thirteen studies published in reputable, peer-reviewed scientific journals within the last decade.

NEURAL HETEROGENEITIES BENEFIT POPULATION CODING AND INFORMATION THROUGHPUT

Population coding involves the integration of stimulus-driven responses from multiple neurons. Individual neurons alone cannot codify all of the complex features of a physiologically relevant stimulus, and thus population coding allows for a more accurate representation of sensory information.⁷ Marsat and Maler (2010) performed *in vivo*, single-cell recordings of a sub-population of pyramidal neurons (known as I-cells) from the electrosensory lateral line lobe (ELL) of weakly-electric fish.⁵ Their results showed that neuronal responses to species-specific, chirping courtship signals vary from I-cell to I-cell, as seen in Figure 1A. Analysis of these heterogeneous responses showed that they improve population coding by minimizing discrimination error from 40% in a homogenous scenario, down to 35% (i.e. where 'discrimination' refers to the ability for I-cells to distinguish between two of these signals), as seen in Figure 1B. They also showed that a small group of heterogeneously-responding I-cells can reliably distinguish these signals.⁵

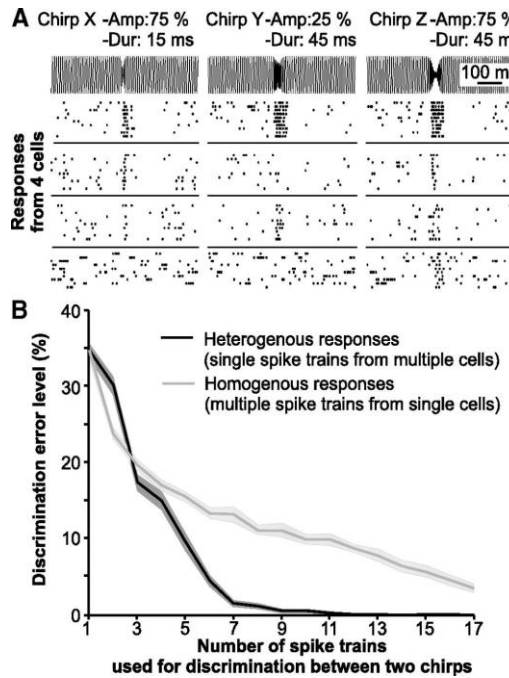


Figure 1: (from Marsat & Maler 2010: Figs. 5A and 5B)

Discrimination of big chirps by I-cells. A: neural responses. We show 3 of the 9 chirps used during the experiment (top traces) followed by raster plots of the responses of 4 cells to several repetitions of the stimulus. These cells were chosen to show the variability in the responses to the chirps within individual pyramidal cells and the much larger variation across cells. We describe the shape of the chirps by their duration (labeled "Dur") and the magnitude of their amplitude decrease (labeled "Amp"). B: mean discriminability ($\pm SE$; $n = 36$ chirp pairs) of responses to different chirps. In our regular analysis, the different responses combined come from different neurons (heterogeneous response, black line), thus assessing the discriminability of the actual population's response. We repeated the analysis combining several responses from the same neuron, thus assessing the discriminability of the responses if the population was homogeneous (gray line).

Ahn et al. (2014) performed *in vitro*, whole-cell patch-clamp recordings of cochlear nucleus angularis (NA) cells in the auditory brainstem of

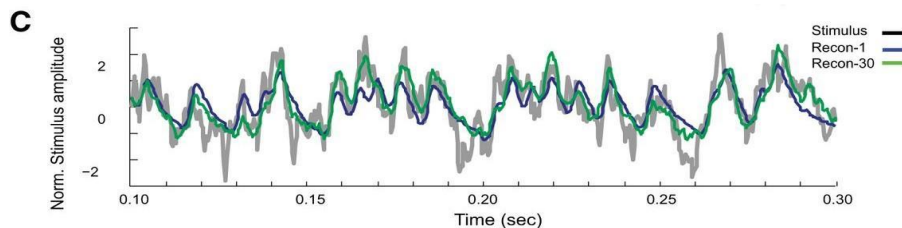


Figure 2 (from Ahn et al. (2014): Fig. 4C) Stimulus reconstruction using reverse correlation noise analysis. Original stimulus current (gray) and the corresponding reconstruction estimates for a typical neuron (Recon-1, blue) or population of 30 neurons (Recon-30, green).

chickens.⁸ Their results showed that heterogeneous spike trains produced by groups of these neurons allowed for a more accurate reconstruction of the stimulus than did spike trains from a single NA neuron (Figure 2 and 3). Stimulus reconstruction (Figure 4) improved with increasing heterogeneity of spike patterns; variations in spike trains across different neurons in a population allowed for codification of a greater proportion of a given stimulus.⁸ Thus, neural heterogeneities benefit population coding by helping to mitigate redundancy and generate more accurate stimulus representations. This result is also supported by Tripathy et al. (2013), who used statistical modeling to show that an intrinsically diverse population of olfactory-bulb mitral cells (MCs) more effectively represents low-frequency stimuli than a homogenous population of the same type of cells.⁹

Chelaru and Dragoi (2008) used computational modeling to show that heterogeneity for orientation-selectivity in layer four neurons of the primary visual cortex mitigates neuronal correlations, which helps to improve efficiency in population coding.¹ Each of these neurons exhibits a unique tuning curve, which shows the orientation of visual input for which that neuron is most active.

Padmanabhan and Urban (2010) performed *in vivo*, whole-cell electrophysiological recordings of MCs located in the mouse olfactory bulb.⁴ Their results showed that heterogeneity in spike patterns allowed for encoding of two-times the amount of information regarding the olfactory stimulus than did homogeneous populations of the same neuron. As seen in Figure 5, a population of neurons that varied in intrinsic biophysical properties carried significantly more information than a population of homogeneous neurons, especially at larger population sizes. This increased information throughput was also conserved when MCs were presented with physiologically relevant, oscillating stimuli (i.e. stimuli from a mouse's sniffing).⁴

To summarize, experimental studies, in addition to computational and statistical models, show that heterogeneities in the intrinsic properties of neurons help to improve population coding of sensory stimuli. When compared to homogeneous populations, those that are heterogeneous in nature exhibit an improved ability to discriminate between like stimuli, more accurate stimulus reconstruction, minimal redundancy, more efficient coding, and an increase in the amount of sensory information encoded by the neurons in the population.

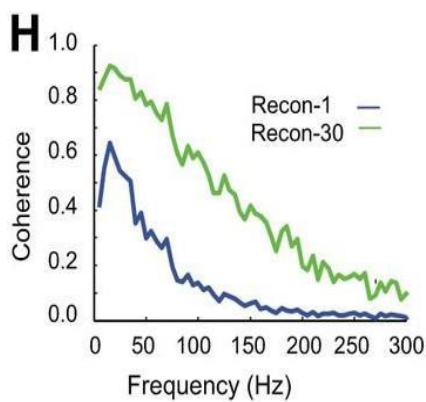


Figure 3 (from Ahn et al. (2014): Fig. 4H) Stimulus reconstruction using reverse correlation noise analysis. coherence of the reconstruction estimates with the original stimulus (blue: single neuron; green: 30 neuron population).

NEURAL HETEROGENEITIES INFLUENCE BURST CODING AND RESPONSES TO ENVELOPES

Avila-Akerberg et al. (2010) performed *in vivo*, single-unit electrophysiological recordings of superficial, intermediate, and deep pyramidal neurons in the ELL of weakly-electric fish in response to local and global electrical stimuli. Local stimuli mimicked prey, whereas global stimuli mimicked conspecific perturbations.¹⁰ These subpopulations of pyramidal neurons were heterogeneous for firing rate; whereas superficial pyramidal neurons exhibited firing rates < 15 Hz, deep pyramidal neurons exhibited firing rates > 30 Hz, and intermediate pyramidal neurons exhibited firing rates within these boundaries. This group also found that superficial and intermediate pyramidal neurons were more likely to burst for local stimuli, whereas deep pyramidal neurons were equally likely to burst for both local and global

stimuli.¹⁰ This result suggests that heterogeneity of firing rate among pyramidal ELL neurons helps weakly-electric fish to encode information regarding threats or other changes in their environment.

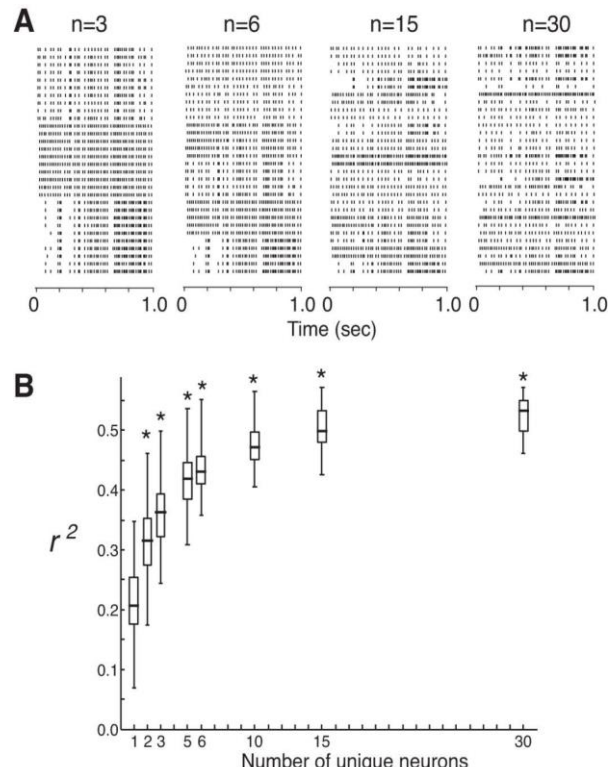


Figure 4 (from Ahn et al. (2014): Figs. 6A and 6B) Population coding improves the stimulus reconstruction. A: population rasters drawn from different neuron pool number for a total of 30 trials show increasing heterogeneity in the firing patterns. B: reconstruction fit (r^2) vs. number of unique neurons in the population group used in the reconstruction estimate ($n = 120$ repeated runs per group containing ≥ 2 unique neurons; $n = 60$ for single-neuron group). Increased heterogeneity results in improved reconstruction fit [one-way ANOVA using Welch's test assuming unequal variances, $F(7,313) = 4.9$, $P < 0.001$; all groups of $n \geq 2$ neurons were significantly different from single-neuron group, * $P < 0.05$, Dunnett multiple-comparisons test]. Box plot represents the median, interquartile range and extrema.

Moreover, Savard et al. (2011) showed that heterogeneities within p-type electro-sensory afferents of gymnotiform weakly-electric fish influence responses to stimulus envelopes.¹¹ P-type afferents are heterogeneous for baseline firing rate; Savard et al. produced results that show a strong, negative correlation between baseline firing

rate and the magnitude of envelope response.¹¹ ON-type, envelope-responsive neurons (i.e., afferents whose response properties are in-phase with the time-varying amplitude of stimuli) had much lower baseline firing rates than OFF-type, non-envelope responsive neurons (whose responses are out-of-phase with stimulus amplitude), suggesting that baseline firing rates might play a role in determining which afferents respond to envelopes and which do not.¹² Interestingly, Metzen and Chacron (2015) showed that a heterogeneous population of p-type afferents, consisting of both ON- and OFF-types, was able to transmit more information regarding fast, time-varying stimuli with a sinusoidal envelope than a population consisting of more ON- or more OFF-type afferents alone.¹²

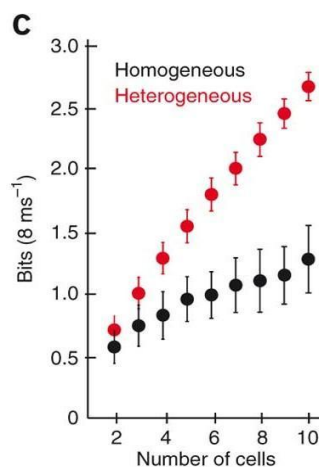


Figure 5 (from Padmanabhan & Urban (2010): Figure 5C) Heterogeneous populations of mitral cells carry twice as much information as homogeneous populations of cells. Error bars represent s.d.

Electrophysiological recordings from weakly-electric fish have allowed researchers to study the heterogeneous response properties of electrosensory neurons to physiologically relevant information. These recordings have shown that firing-rate heterogeneities in ELL pyramidal neurons help to encode various electrical stimuli in the fish's environment through bursts of action potentials. Furthermore, we see that firing-rate heterogeneities in P-type electrosensory afferents help to encode information regarding the envelope of a stimulus.

HETEROGENEITIES HAVE DIFFERENTIAL EFFECTS AMONG EXCITATORY AND INHIBITORY NEURONS

Mejias and Longtin (2014) used analytical and mathematical models to show that heterogeneities among excitatory and inhibitory neurons have different consequences for information processing.¹³ In a sparsely-connected cortical circuit consisting of both an excitatory and an inhibitory component (arising from pyramidal and interneurons, respectively), we see different effects of heterogeneity. Specifically, the researchers found that heterogeneity among excitatory neurons increases the mean firing rate of the entire cortical network and generates a linear input-output frequency-current (f-I) curve.¹³ Conversely, heterogeneity among inhibitory neurons may decrease the activity of the cortical network; this then divisively influences the gain of excitatory f-I curves.

CONCLUSION

While neural heterogeneities have been documented in many different contexts and cell types, there still remains much to be discovered regarding their specific functions in the neural code. The current state of scientific knowledge, which has been derived from experimental research and theoretical modeling, suggests that heterogeneities in the intrinsic properties of a given neuronal cell type facilitate processing of sensory information. This summary has discussed the role of neural heterogeneities in population coding, which allow for more accurate representations of sensory stimuli than any single neuronal response. Specific experiments have demonstrated this to be true in their ability to increase information throughput, shape burst coding of physiologically relevant stimuli, represent sinusoidal envelopes of stimuli, and to elicit differential excitatory and inhibitory effects on the basic cortical circuit.

REFERENCES

- Chelaru MI, Dragoi V. Efficient coding in heterogeneous neuronal populations. Proc Natl Acad Sci U S A. 2008 Oct 21; 105(42):16344-9.
- Marder E, Goaillard JM. Variability, compensation and homeostasis in neuron and network function. Nat Rev Neurosci. 2006 July; 7(7):563-74.

3. Shulz DJ, Goaillard JM, Marder E. Variable channel expression in identified single and electrically coupled neurons in different animals. *Nat Neurosci.* 2006 Mar; 9(3):356-62.
4. Padmanabhan K, Urban NN. Intrinsic biophysical diversity decorrelates neuronal firing while increasing information content. *Nat Neurosci.* 2010 Oct; 13(10):1276-82.
5. Marsat G, Maler L. Neural heterogeneity and efficient population codes for communication signals. *J Neurophysiol.* 2010 Nov; 104(5):2543-55.
6. Angelo K, Margrie TW. Population diversity and function of hyperpolarization-activated current in olfactory bulb mitral cells. *Sci Rep.* 2011; 1:50.
7. Averbeck BB, Latham PE, Pouget A. Neural correlations, population coding and computation. *Nat Rev Neurosci.* 2006 May; 7(5):358-66.
8. Ahn J, Kreeger LJ, Lubejko ST, Butts DA, MacLeod KM. Heterogeneity of intrinsic biophysical properties among cochlear nucleus neurons improves the population coding of temporal information. *J Neurophysiol.* 2014 Jun 1; 111(11):2320-31.
9. Tripathy SJ, Padmanabhan K, Gerkin RC, Urban NN. Intermediate intrinsic diversity enhances neural population coding. *Proc Natl Acad Sci U S A.* 2013 May 14; 110(20):8248-53.
10. Avila-Akerberg O, Krahe R, Chacron M. Neural heterogeneities and stimulus properties affect burst coding *in vivo*. *Neuroscience.* 2010 Jun 16; 168(1):300-13.
11. Savard M, Krahe R, Chacron MJ. Neural heterogeneities influence envelope and temporal coding at the sensory periphery. *Neuroscience.* 2011 Jan 13; 172:270-84.
12. Metzen MG, Chacron MJ. Neural Heterogeneities Determine Response Characteristics to Second-, but Not First-Order Stimulus Features. *J Neurosci.* 2015 Feb 18; 35(7):3124-38.
13. Mejias JF, Longtin A. Differential effects of excitatory and inhibitory heterogeneity on the gain and asynchronous state of sparse cortical networks. *Front Comput Neurosci.* 2014 Sept 12; 8:107.

The Authors

Kavya Anchuri



Kavya is a U3 student who feels fortunate to have spent three rigorous, challenging, and intellectually stimulating years in the Physiology department at McGill. She has particularly enjoyed seminar-style courses, such as PHGY 524, which delved into the genetic and molecular underpinnings of circadian rhythms. Kavya hopes to begin a Master of Public Health in the fall, having received offers from both McGill and Yale University.

Aleksandar Borisov



Aleksandar is a U3 Physiology student currently completing an Honours Research Project in the Alvin Shrier lab, studying the effects of a serotonin antagonist drug on the hERG delayed rectifier potassium channel – which is responsible for heart repolarization. Throughout his time in the Shrier lab, Aleksandar has learned various electrophysiological techniques, including manual whole cell patch clamping. He has also had experience working in a microscopy laboratory, studying cellular dynamics in relation to cancer metastasis. Aleksandar is an author, as well as an editor for this publication of JUMPS, and is an aspiring cardiologist and professional beach volleyball athlete.

Hannah Kapur



Hannah is a U3 Physiology major with a minor in Kinesiology. She completed a summer studentship and independent research project in a human genetics lab studying pediatric brain tumours at the McGill University Health Centre (MUHC). Hannah completed her research alongside a postdoctoral fellow in the lab. Together, they investigated the effects of epigenetic probes (small molecule inhibitors) on various patient-derived glioblastoma cell lines in order to discover therapeutic targets. Hannah really enjoyed her time in the lab, and she thought it was an excellent introduction to research. She has always had a keen interest for research, and she started the McGill Undergraduate Physiology Students Journal Club in 2015. This is actually Hannah's second appearance in JUMPS as she was the first co-author on a paper the Journal Club submitted last year. Hannah also competed on the McGill Varsity Alpine Ski Team throughout her undergraduate career, and she was Captain of the team this past year. In her free time, Hannah enjoys volunteering at the Montreal General Hospital and hanging out with her Best Buddy, as well as working out and exploring the city and travelling the east coast when she can (Hannah is from the west and doesn't think the east coast is the least coast!).

The Editors

Ryan Buyting



Ryan is a U3 student in the Physiology Major program at McGill, and served as the PULS Charity Director for the 2016-17 school year. His past clinical research has involved developing a risk stratification method for thromboembolic events occurring in multiple myeloma patients, as well as examining the efficacy of reversal agents used to treat patients with bleeding complications while prescribed anticoagulants. This work lead to authorships in the Blood Journal, and the Journal of Thrombosis and Haemostasis. Ryan worked in Dr. Marie Trudel's Molecular Genetics and Development laboratory during his graduating year, where he studied hemoglobin disorders and the genes that may play a role in them. Additionally, he served as a manuscript editor for Dr. Amir Shmuel, contributing to papers in the field of neuronal fMRI technology, prior to their publication.

Vivian Tse



Vivian is a U3 student in the Honours Physiology program. Her research interest lies in the interdisciplinary area between physiology and quantitative sciences. In the past, she was involved in developing a better assay to measure traction forces produced by cells and investigating biophysical properties of aging cells. Currently, her current research thesis project is looking at Polycystin 2 gating on stretch activated ion channels and membrane tension. It is a collaboration between Professor Reza Sharif-Naeini from the department of physiology and Professor Allen Ehrlicher from the department of bioengineering. Vivian hopes that JUMPS will provide an opportunity for more undergraduates to participate in the research community.

Vasikar Murugapoopathy



Vasikar is a U3 Student in the Honours Physiology program. He has worked in Dr. Indra Gupta's lab for almost two years with research interests in pediatric nephrology, and development of the urinary system leading to a publication in the American Journal of Physiology. His current research project focuses on the use of transcriptomic analysis to identify novel genes underlying the development of Vesico-ureteral Reflux, one of the most common disorders in children. After completing his undergrad, Vasikar plans on starting a Masters in Human Genetics at McGill University to build on his honors project.

Parmida Parsa



Parmida is a U2 Physiology student. She's quickly appreciated the advancements into the understanding of physiological systems research can bring. Her past research interests have included wound healing and chronic pain in rheumatoid arthritis. She hopes that JUMPS can give recognition to passionate undergraduate student researchers as well as encourage new students to get involved.

Jack Mouhanna



Jack is a U3 Honours Physiology student and has been involved in research since his first year at McGill in cancer immunology and biomedical engineering. His current research focuses on exploring the role of neutrophils in cancer metastasis by examining neutrophil trafficking near early metastatic implants. Having had a meaningful, rewarding experience, Jack encourages undergraduate students to explore their interest in research through the many opportunities that exist here at McGill. Jack hopes that JUMPS will continue to promote undergraduate research by inspiring students to get involved in research early on in their careers.

Armon Hadian



Armon is a U3 Honours Physiology student who first delved into research in the summer of his first year, editing manuscripts for the a mental health research team at the IWK hospital in Halifax. He began his research at McGill working on the optimization of antibody protocols, employing confocal and high-content screening microscopy. He then received a GEPROM grant in the summer of 2016 and worked on using rapid line scanning confocal microscopy to reduce phototoxicity during fluorescent imaging. He is currently working in Dr. Orlowski's lab on a project regarding the molecular mechanisms underlying NHE6 misregulation in Christianson Syndrome patients.

Design and Formatting

Jiachen Liang



Jiachen is a U3 physiology student with interests rooted in cell and molecular physiology, and cancer biology. He took on two research projects in his degree. In Dr. Julie St-Pierre's laboratory, he studied the action of metformin, an ETC complex I inhibitor, on the role of PGC-1 in metastatic breast cancer. He then went to work with Dr. Alvin Shrier on the degradation of mutant hERG channels. Although his research is heavily molecular, he encourages undergraduate students to pick up computer skills while at McGill, just like he did. *In silico* is the next big step, and to have knowledge of bioinformatics will come in handy in the very near future.

